

## Role of percolation in diffusion on random lattices

Andreas Hörner

*Institut für Physik, Max-Planck-Institut für Metallforschung, D-70569 Stuttgart, Germany*

Andrey Milchev

*Institute for Chemical Physics, Bulgarian Academy of Sciences, 1040 Sofia, Bulgaria*

Panos Argyrakis

*Department of Physics, University of Thessaloniki, 54006 Thessaloniki, Greece*

(Received 11 January 1995)

Diffusion of single particles on lattices with random distributions of static barriers (random-barrier model) is investigated by Monte Carlo simulations and the time-dependent effective-medium approximation. The crossover from anomalous to linear diffusive behavior is discussed in terms of a percolation model. For a discrete distribution of barrier heights with a small concentration of “defect” barriers at the percolation threshold, an alternative kind of transition from bulk-controlled to defect-controlled diffusion is observed as the temperature decreases.

PACS number(s): 05.40.+j, 66.30.Dn, 05.60.+w

### I. INTRODUCTION

Amorphous solids and other disordered systems often exhibit transport via the hopping mechanism such as hopping transport in semiconductors, ionic conductivity in superionic solids, carrier recombination in glasses, and dispersion (mixing) in flow through porous media. It is well known that transport properties behave irregularly in such cases, leading to anomalous diffusion such as Brownian particles [1]. As a rule, the medium may be considered statistically disordered as in ordinary bond percolation, whereby the hopping particle performs thermally activated jumps along easy paths (channels) which are open or closed with a certain probability, due to a random distribution of the potential barriers. In what follows we shall consider the so-called *random-barrier* model [2] in which the potential minima at the lattice sites are constant whereas the potential barriers between the sites are chosen from a uniform distribution.

In two and three dimensions, large barriers can be circumvented easily, so that the particle may find an unblocked path from one end of the medium to the other. This macroscopic diffusion path will span an infinite cluster of low-enough adjacent barriers between sites and will be characterized by some *effective* activation energy barrier  $E_p$ , which should generally coincide with the highest barrier along the diffusion path [3,4]. It is to be expected that on finite fractions of this percolating cluster the occurrence of lower barriers will cause the motion of the hopping particle to be confined within such fractions and be highly correlated (anomalously diffusive). However, if the mean-square displacement (MSD) is measured in units of the average residence time  $t_c$  in such low-barrier basins, one should observe Fick’s law  $\langle r^2 \rangle \propto t$ . The mean stay time  $t_c$  in the low-energy basins will grow with de-

creasing temperature  $T$ , and by studying the  $t_c - T$  relationship one should be able, at least in principle, to recover the critical concentration  $p_c$  of easy channels in the underlying lattice [4,5]. The idea of the existence of a critical path for particle diffusion in a disordered medium was first explored by Mott [6], and then extended by Ambegekar, Halperin, and Langer [3], who studied hopping conductivity of electrons. This was done by treating hopping as tunneling of the electrons between localized states that are randomly distributed in the lattice, thus mapping this problem to an effective percolation problem. In that study [3] they calculated the effective conductance, which gave  $G_c$  critical values very close to the geometric percolation values, as also shown by our present model [4].

In the present paper we investigate the problem by means of Monte Carlo (MC) simulation and the effective medium approximation (EMA), and demonstrate that the results of both methods comply with the considerations given above. Having thus established the reliability of the EMA approach, which requires computationally much less effort, we consider in detail the behavior of the system in the vicinity of the percolation threshold  $p_c$  using a *ternary* distribution of energy barriers of three fixed heights. The concentrations of barriers, which are chosen considerably lower or higher than  $E_p$ , are kept slightly below  $p_c$ . This is done so that one may be able to carefully examine the role of a third sort of barrier (which we call hereafter “defect” barriers), in a concentration closing the gap to  $p_c$ .

The organization of the present paper is as follows: in Sec. II we present the MC method and the results derived from the MC simulations, whereas in Sec. III we briefly recall the main premises of the EMA. A comparison of the MC and EMA results is presented in Sec. IV and in Sec. V we give a brief summary of the present investigations.

## II. THE MONTE CARLO SIMULATION

In the present investigation, as in an earlier work [4], the random barriers define transition rates

$$J_{ij} = (\nu_0/Z) \exp(-E_{ij}/k_B T) \quad (1)$$

that are governed by Boltzmann statistics in standard fashion. Here  $\nu_0$  denotes the constant jump rate and  $Z$  is the coordination number of the lattice. A common point of departure for many theoretical investigations of stochastic transport is the master equation

$$\frac{\partial}{\partial t} P(\mathbf{r}_i, t) = \sum_{j \in \{i\}} [J_{ji} P(\mathbf{r}_j, t) - J_{ij} P(\mathbf{r}_i, t)], \quad (2)$$

which can be viewed as the description of the motion of a particle on a lattice.  $P(\mathbf{r}_i, t)$  is the probability of finding the particle at site  $i$  at time  $t$ . We impose the restriction that jumps made between two specific sites carry exactly the same transition rates at any time during the calculation,  $J_{ij} = J_{ji}$ . For example, once a forward jump is made in a particular direction, then the backward jump (back to the original position) should carry the same probability as the forward jump. A random distribution of jump rates arises then from a random distribution  $\rho(E)$  of potential barriers of height  $E$  (in this paper we employ dimensionless units for the energy whereby the temperature  $T$  is measured in units of  $E_{max}/k_B$  with  $E_{max} = 1$ ). Therefore, we use a model where the barrier energies are defined by use of the equation

$$\rho(E) = \begin{cases} 1 & \text{for } E \in [0, 1] \\ 0 & \text{otherwise.} \end{cases} \quad (3)$$

The transition rates may be converted into probabilities by dividing them by  $\nu_0$ . After all  $J$ 's are summed up, the remainder to 1 becomes the probability  $J_{ii}/\nu_0$ :

$$J_{ii}/\nu_0 = 1 - \sum_{i \neq j} J_{ij}/\nu_0, \quad (4)$$

for the particles to remain on the same site.

Calculations have been carried out on two-dimensional (2D) square lattices (four nearest neighbors), and on 3D simple cubic lattices (six neighbors). More details about the MC procedure may be found in our earlier work [4].

Figure 1 describes the behavior of the MSD in 2D,  $\langle r^2 \rangle$ , as a function of time at different temperatures. We present data for the range  $10-10^7$  steps. Similar calculations, but in 3D, are shown in Fig. 2. Both in 2D and in 3D we observe that for all temperatures there is always an early-time regime that differs from the diffusive regime  $\langle r^2 \rangle \propto Dt$ , i.e., at each temperature there is a particular crossover time  $t_c$  denoting the transition from anomalous to normal diffusive motion, the latter being clearly seen on the log-log plots as a linear relationship at late times. As the temperature decreases, linearity is achieved at longer and longer times  $t_c$ . We find that the crossover time varies with  $T$  as

$$t_c \propto \exp(E_p/k_B T), \quad (5)$$

where  $E_p$  defines some effective activation energy. Indeed, one can estimate the crossover time  $t_c$  for each temperature and plot it versus  $1/T$  in lin-log fashion as shown in Fig. 3 for both the 2D and 3D lattices. The slope of the line is  $E_t = 0.518$  (2D) and  $E_t = 0.293$  (3D).

## III. EFFECTIVE-MEDIUM APPROXIMATION

### A. Method

Another approach to the calculation of the mean-square displacement of a particle on a lattice with static random barriers is represented by the effective-medium

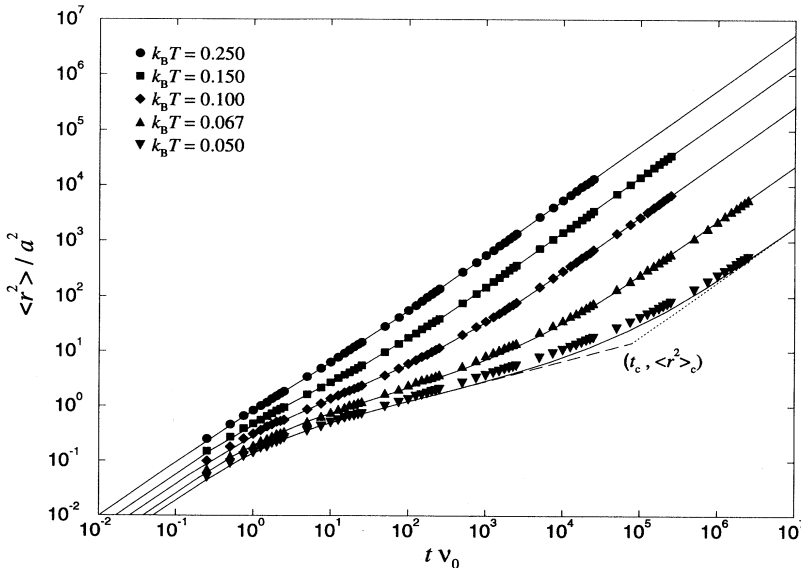


FIG. 1. MSD of a particle as a function of time on a square lattice with the distribution of barrier heights, given in Eq. (3); MC simulations (symbols) and EMA (solid lines); intersecting lines are the tangent in the turning point (dashed line) and the long-time asymptote (dotted line) of the MSD for  $k_B T = 0.05$ .

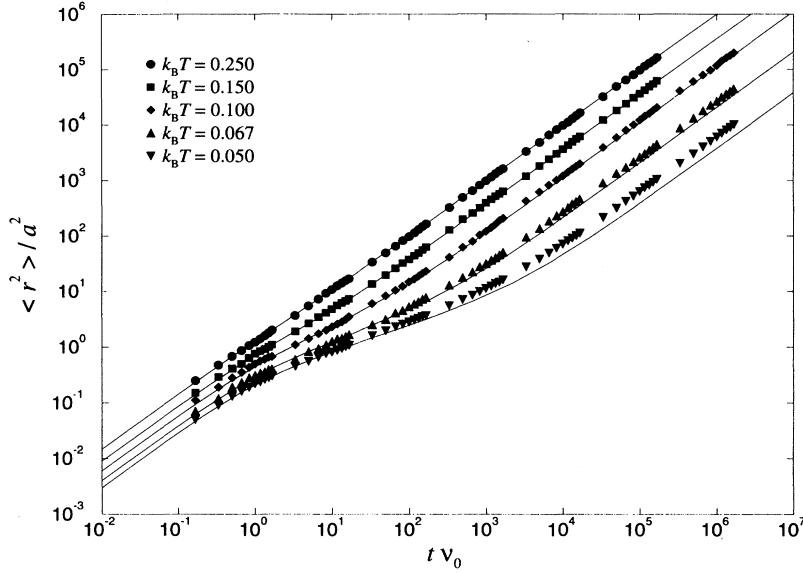


FIG. 2. Same as Fig. 1, on a simple cubic lattice.

approximation [2,7–9], which was developed originally [10] for description of the dc conductivity of a random resistor network. This approach was generalized [7–9] to the ac case by means of a coherent potential approximation in which a kind of a scattering  $T$  matrix produced by a disordered unit embedded in a coherent medium is forced to be zero on average to self-consistently determine the coherent medium and hence the coherent transition probability. When applied to hopping conduction problems in topologically disordered systems, the method reflects the existence of a percolation threshold when an infinite cluster of conducting bonds spans the system. The scheme followed by EMA is the following: After performing the Laplace transform of Eq. (2), which yields

$$s\tilde{P}(\mathbf{r}_i, s) - \delta_{i,0} = \sum_{j \in \{i\}} [J_{ji}\tilde{P}(\mathbf{r}_j, s) - J_{ij}\tilde{P}(\mathbf{r}_i, s)], \quad (6)$$

and averaging over all configurations of jump frequencies (indicated by the brackets), the set of static local jump frequencies  $\{J_{ij}\}$  is replaced by a single position-independent, but frequency-dependent, effective jump frequency  $J_c$ :

$$s\langle \tilde{P}(\mathbf{r}_i, s) \rangle - \delta_{i,0} = J_c(s) \sum_{j \in \{i\}} [\langle \tilde{P}(\mathbf{r}_j, s) \rangle - \langle \tilde{P}(\mathbf{r}_i, s) \rangle]. \quad (7)$$

From the solution of this equation the Laplace transformed MSD is obtained as

$$\langle r^2 \rangle(s) = Za^2 \tilde{J}_c(s) / s^2, \quad (8)$$

where  $a$  denotes the lattice constant. In principle, the effective jump frequency  $\tilde{J}_c$  is to be determined from the self-consistency condition

$$\langle \tilde{P}(\mathbf{r}_i, s) \rangle_{\{J_{ij}\}} = \tilde{G}(\mathbf{r}_i, s, \tilde{J}_c), \quad (9)$$

where  $\tilde{G}(\mathbf{r}_i, s, \tilde{J}_c)$  is the Laplace transformed sojourn probability in an effective medium with the spatially constant jump frequency  $\tilde{J}_c$ . Because it is impossible to express the configurational average over all (i.e., an infinite number of) local jump frequencies as a function of the  $\tilde{G}(\mathbf{r}_i, s, \tilde{J}_c)$  and to solve for  $\tilde{J}_c$ , one is forced to use an approximation. In the EMA, the real system is replaced by another one with only a small cluster of fluctuating jump frequencies  $\{J_{mn}\}$ ; all other jump frequencies are assigned the value  $\tilde{J}_c$ . In this system, the configurational average  $\langle \tilde{P}^*(\mathbf{r}_i, s) \rangle_{\{J_{mn}\}}$  can be written as a function of  $\tilde{G}(\mathbf{r}_i, s, \tilde{J}_c)$ , and  $\tilde{J}_c$  can be obtained from the new self-consistency conditions

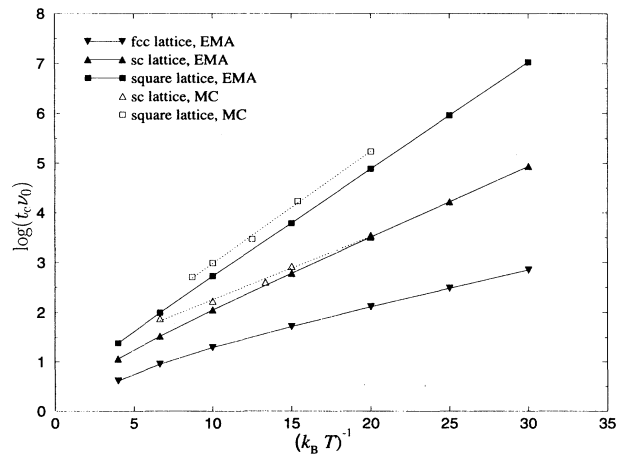


FIG. 3. Crossover times as a function of reciprocal temperature for diffusion on various lattices, with the distribution of barrier heights given in Eq. (3); MC simulations (hollow symbols) and EMA (full symbols). The slopes of the MC data (dotted lines) are 0.293 for the simple cubic and 0.518 for the square lattice. Lines are guides for the eye. The  $y$  axis is a  $\log_{10}$  axis.

$$\langle \tilde{P}^*(\mathbf{r}_i, s) \rangle_{\{J_{mn}\}} = \tilde{G}(\mathbf{r}_i, s, \tilde{J}_c). \quad (10)$$

Within the simplest approximation suitable for a random-barrier model, the so-called single-bond EMA, a single jump frequency  $J_\alpha$  between a pair of neighboring places (i.e., a single barrier height) is allowed to fluctuate. In this case, the set of equations (10) reduces to the self-consistency condition

$$\left\langle \frac{J_\alpha - \tilde{J}_c}{1 - 2[s\tilde{G}(\mathbf{0}, s) - 1](J_\alpha - \tilde{J}_c)/(z\tilde{J}_c)} \right\rangle_{J_\alpha} = 0, \quad (11)$$

where the brackets symbolize the average over the distribution of jump frequencies  $J_\alpha$  (which corresponds to a distribution of barrier heights). The value of  $\tilde{G}(\mathbf{0}, s)$  depends on lattice structure; it is given by

$$\tilde{G}_{sq}(\mathbf{0}, s) = (1/2\pi)^2 \tilde{J}_c^{-1} \int_{-\pi}^{\pi} \int_{-\pi}^{\pi} \frac{d\kappa_1 d\kappa_2}{s/\tilde{J}_c + 4 - 2 \cos \kappa_1 - 2 \cos \kappa_2} \quad (12)$$

for a square lattice, by

$$\tilde{G}_{sc}(\mathbf{0}, s) = (1/2\pi)^3 \tilde{J}_c^{-1} \int_{-\pi}^{\pi} \int_{-\pi}^{\pi} \int_{-\pi}^{\pi} \frac{d\kappa_1 d\kappa_2 d\kappa_3}{s/\tilde{J}_c + 6 - 2 \cos \kappa_1 - 2 \cos \kappa_2 - 2 \cos \kappa_3} \quad (13)$$

for a simple cubic lattice, and by

$$\tilde{G}_{fcc}(\mathbf{0}, s) = (1/2\pi)^3 \tilde{J}_c^{-1} \int_{-\pi}^{\pi} \int_{-\pi}^{\pi} \int_{-\pi}^{\pi} \frac{d\kappa_1 d\kappa_2 d\kappa_3}{s/\tilde{J}_c + 12 - 4(\cos \kappa_1 \cos \kappa_2 + \cos \kappa_2 \cos \kappa_3 + \cos \kappa_3 \cos \kappa_1)} \quad (14)$$

for a face-centered cubic lattice.

From Eq. (11), series expansions for the MSD have been derived in the limit of short and long diffusion times [2]. Since we are interested in the evolution of the MSD in the crossover region, i.e., at intermediate times, we chose to perform the inverse Laplace transform of Eq. (8) numerically. This requires knowledge of  $\tilde{J}_c(s)$  for complex arguments  $s$ , which is obtained by iterative solution of Eq. (11). Within each iteration step,  $\tilde{G}(\mathbf{0}, s)$  has to be calculated by numerical integration of Eqs. (12) and (13) or Eq. (14) for the current value of  $\tilde{J}_c$ .

Following this scheme, we arrive at the time-dependent MSD of a particle, as by use of the MC technique described in the last chapter, but with considerably less computational effort and without statistical errors. However, systematic errors are introduced by the EMA, so that its applicability has to be established by comparison with results from alternative methods, as will be done in the following section.

## B. Results

The time-dependent EMA, described above, was used to calculate the MSD of particles in the same random-barrier models as treated by MC simulations. The results are given as solid lines in Figs. 1 and 2. Evidently, EMA and MC results agree well within the time range accessible to both methods, which shows the systematic errors of the former and the statistical errors of the latter method to be reasonably small. We notice that there are deviations [11] between the EMA results and the numerical simulations at low temperature which persist in the long-time regime in  $D = 3$ , but not in  $D = 2$ . Luck [12] considered the difference between the EMA and an exact perturbation expansion.

The temperature dependence of  $t_c$  according to EMA

and MC calculations for the square and simple-cubic lattices are summarized in Fig. 3, together with EMA results for the face-centered cubic lattice with the same distribution of barrier heights. For low temperatures,  $t_c$  obeys an Arrhenius law, Eq. (5). The activation energies  $E_p$  are 1/2, 1/3, and 1/6 for the square, simple cubic, and fcc lattices, respectively. These values are easily interpreted, if we change our point of view and have a look at ‘‘crossover mean-square displacement’’  $\langle r^2 \rangle_c$ , which is the MSD coordinate of the point used for determination of  $t_c$ . Since the distribution of barrier heights is the same for all temperatures,  $\langle r^2 \rangle_c$  is expected to be an almost constant function of  $T$ , which is indeed the case (see Fig. 4).  $\langle r^2 \rangle_c$  being independent of temperature,  $t_c$  is determined

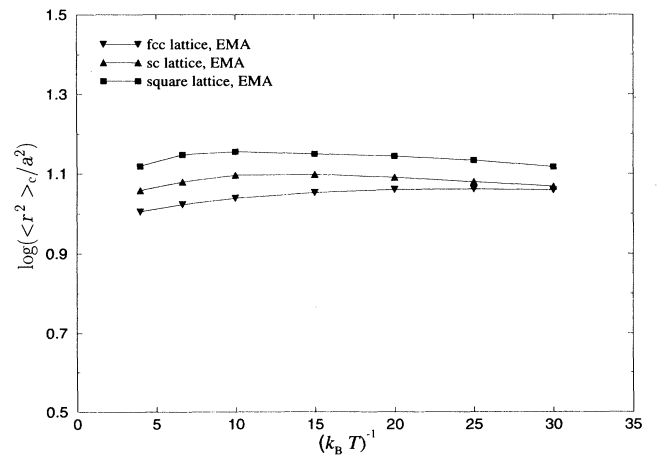


FIG. 4. Crossover MSD as a function of reciprocal temperature for diffusion on different lattices, with the distribution of barrier heights given in Eq. (3); symbols: calculated by EMA. Lines are guides for the eye.

by the long-time asymptote of the MSD alone; thus  $t_c$  is reciprocal to the effective jump frequency  $J_c^l$  in the limit of long diffusion times.  $J_c^l$  of a random-barrier model in more than one dimension is known, within EMA, to obey an Arrhenius law for low temperatures [13]

$$J_c^l \sim \exp[-E_p/(k_B T)] \quad (15)$$

so that the Arrhenius behavior of  $t_c$  is a direct consequence of the temperature dependence of  $J_c^l$ . The activation energy  $E_p$  corresponds to the height of those barriers that represent the threshold for bond percolation:

$$\int_{E=0}^{E_p} \rho(E) dE = p_c^{EMA} = 2/Z, \quad (16)$$

where  $p_c$  is the EMA bond percolation concentration [2]. Schirmacher [13] gives the following illustrative explanation: At low temperatures, all barriers higher than  $E_p$  are effectively insurmountable. Jumps over barriers lower than  $E_p$  are very frequent, but do not result in long-range diffusion, because there are only finite clusters of lattice sites connected by these low barriers. Thus, the barriers of height  $E_p$  control the temperature dependence of  $J_c^l$ . Solving Eq. (16) for the box distribution of barrier heights Eq. (3), one arrives at the activation energies  $2/Z$  mentioned above. Since the real percolation concentrations are lower than the EMA values [2] (with the exception of the square lattice, where EMA supplies the correct value  $1/2$ ), the activation energies obtained by MC simulations are expected to be lower than  $2/Z$  and this is indeed observed in 3D where the measured slope is 0.293.

Having thus established both the usefulness of EMA and the importance of percolation for continuous distributions of barrier heights, we now turn to a discussion of EMA results for the *ternary* distribution

$$\rho(E) = \delta(E_l)(1 - \epsilon)/2 + \delta(E_\epsilon)\epsilon + \delta(E_h)(1 - \epsilon)/2, \quad (17)$$

with  $E_l < E_\epsilon < E_h$ , on a square lattice. Since the bond percolation concentration of the square lattice is  $1/2$  (EMA and exact), the defect barriers of height  $E_\epsilon$  and (small) concentration  $\epsilon \ll 1$  close the percolation path. Although EMA fails to give quantitatively exact results in the critical region of a percolation transition, we expect the remarkable behavior of diffusion in this model, predicted by EMA, to be qualitatively correct. We calculated  $\langle r^2 \rangle(t)$  for a wide range of temperatures and concentrations  $\epsilon$ ; Figs. 5–7 show results for the choice  $E_l = 0.1$ ,  $E_\epsilon = 0.7$ , and  $E_h = 0.9$ .

We first focus on the case  $\epsilon = 0$ , where there are only two kinds of barriers, both at the percolation concentration. Looking at Fig. 5, we distinguish three different regions (I, II, III) in the evolution of the MSD, as in the case of continuous distributions of barrier heights: In the short-time regime I, the MSD grows linearly in time, proportionally to the short-time effective jump frequency  $J_c^s$ , which is just the arithmetic mean of the jump frequencies  $J_l$  and  $J_h$  derived from the barrier heights  $E_l$  and  $E_h$ , according to (7). For low temperatures,  $J_h \ll J_l$  can be neglected in taking the average; then the relation

$$J_c^s \sim \exp[-E_l/(k_B T)] \quad (18)$$

holds, reflecting the nearly normal diffusive movement the particle initially performs until the borders of the easy-path region are reached.

In the long-time regime III, the MSD grows linearly, too, proportionally to the long-time effective jump frequency  $J_c^l$ , which is reduced with respect to  $J_c^s$  by the correlations between successive jumps of the particle. With

$$\lim_{s \rightarrow 0} s \tilde{G}(\mathbf{0}, s) = 0, \quad (19)$$

which holds for all types of lattices, Eq. (11) becomes

$$\left\langle \frac{J_\alpha - J_c^l}{J_\alpha + (Z/2 - 1)J_c^l} \right\rangle_{J_\alpha} = 0 \quad (20)$$

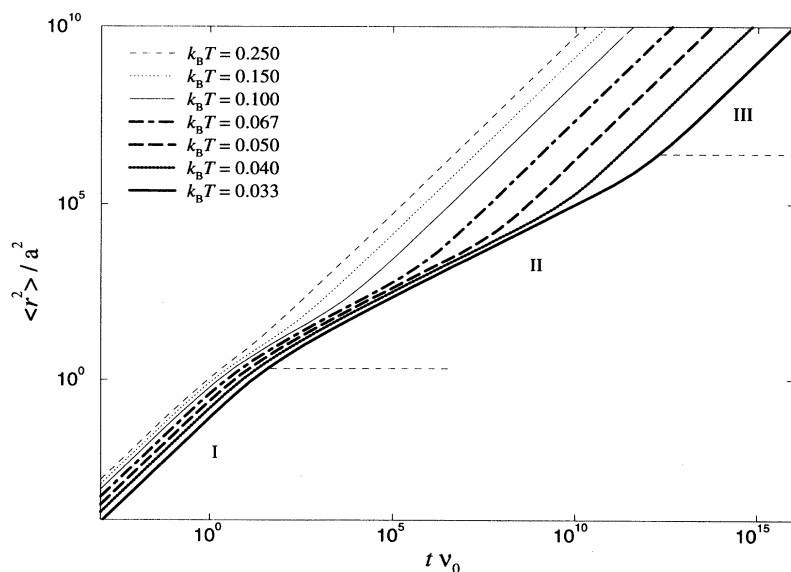


FIG. 5. MSD of a particle as a function of time on a square lattice with the distribution of barrier heights, given in Eq. (17), for  $\epsilon = 0$ , as calculated by EMA; horizontal dashed lines separate regions I, II, III in the case  $k_B T = 0.033$ .

in the long-time limit. For a square lattice and distribution (17), we have

$$1 - \frac{J_l}{J_l + J_c^l} - \frac{J_h}{J_h + J_c^l} + \epsilon \left( \frac{J_l}{J_l + J_c^l} + \frac{J_h}{J_h + J_c^l} - 2 \frac{J_\epsilon}{J_\epsilon + J_c^l} \right) = 0. \quad (21)$$

The positive real root of Eq. (21) for  $\epsilon = 0$  is

$$J_c^l = (J_l J_h)^{1/2}, \quad (22)$$

which is the geometrical mean of the jump frequencies and coincides with the exact result [14]. Its temperature dependence is given by

$$J_c^l \sim \exp \left( -\frac{E_l + E_h}{2k_B T} \right). \quad (23)$$

At intermediate times (region II), diffusion gradually slows down, which leads to a sublinear behavior of the MSD; it grows according to a power law  $\langle r^2 \rangle \sim t^\alpha$ . From Fig. 5 we derive  $\alpha \approx 0.53$  for all temperatures.

By definition, the crossover MSD  $\langle r^2 \rangle_c$  is the upper boundary of region II. In contrast to the findings for the continuous distribution, discussed above, in this case  $\langle r^2 \rangle_c$  varies with temperature, because here no barrier height is unambiguously assigned to the percolation concentration. Thus, the crossover MSD is not determined by some average cluster size but by the difference of the discrete jump frequencies, which grows with decreasing temperature. We give an estimation of its temperature dependence in the low-temperature region by comparing two MSD isotherms belonging to temperatures  $T_1$  and  $T_2 < T_1$ . We know from Eq. (18) that

$$\ln t_2 \langle r^2 \rangle - \ln t_1 \langle r^2 \rangle = E_l \frac{t_1 - t_2}{k_B T_1 T_2} \quad (24)$$

in region I; we know from (23) that

$$\ln t_2 \langle r^2 \rangle - \ln t_1 \langle r^2 \rangle = (E_l + E_h) \frac{T_1 - T_2}{2k_B T_1 T_2} \quad (25)$$

when region III has been reached at both temperatures. Approximating the course of MSD in region II by a straight line with slope  $\alpha$  in a log-log plot and assuming that region II starts at the same MSD for all temperatures, we obtain the result

$$\ln \langle r^2 \rangle_{c,2} - \ln \langle r^2 \rangle_{c,1} = \alpha (E_h - E_l) \frac{T_1 - T_2}{k_B T_1 T_2 (2 - 2\alpha)}. \quad (26)$$

Consequently,  $\langle r^2 \rangle_c$  obeys, for low temperatures, an Arrhenius law

$$\langle r^2 \rangle_c \sim \exp \left\{ \alpha \frac{(E_h - E_l)}{k_B T (2 - 2\alpha)} \right\}. \quad (27)$$

With our actual choice of parameters, the activation energy of this Arrhenius law,  $\alpha \frac{E_h - E_l}{2 - 2\alpha}$ , is approximately equal to 0.45, which is indeed the asymptotic activation energy of the crossover MSD for  $\epsilon = 0$  in Fig. 7. Since the long-time effective jump frequency varies according to Eq. (23), the crossover time  $t_c$  obeys an Arrhenius law with the activation energy  $\frac{E_h - (2\alpha - 1)E_l}{2 - 2\alpha}$ .

We are now prepared to interpret the behavior of diffusion for  $\epsilon > 0$  (see Figs. 6 and 7). Since the concentration of low barriers is now less than the percolation concentration, long-range diffusion is impossible without jumps over barriers of height  $E_\epsilon$ . These barriers at the percolation threshold separate finite clusters of lattice sites with low barriers between them. The average size of these clusters determines an upper limit  $\langle r^2 \rangle_{c,d}$  for the crossover MSD. At sufficiently high temperatures or low  $\epsilon$ ,  $\langle r^2 \rangle_c(\epsilon = 0)$  is smaller than that limit, so the MSD behaves as in the case  $\epsilon = 0$ , and diffusion is controlled entirely by the "bulk properties"  $E_l$  and  $E_h$ . At low temperatures or high  $\epsilon$ ,  $\langle r^2 \rangle_c(\epsilon = 0)$  exceeds  $\langle r^2 \rangle_{c,d}$ ; then,

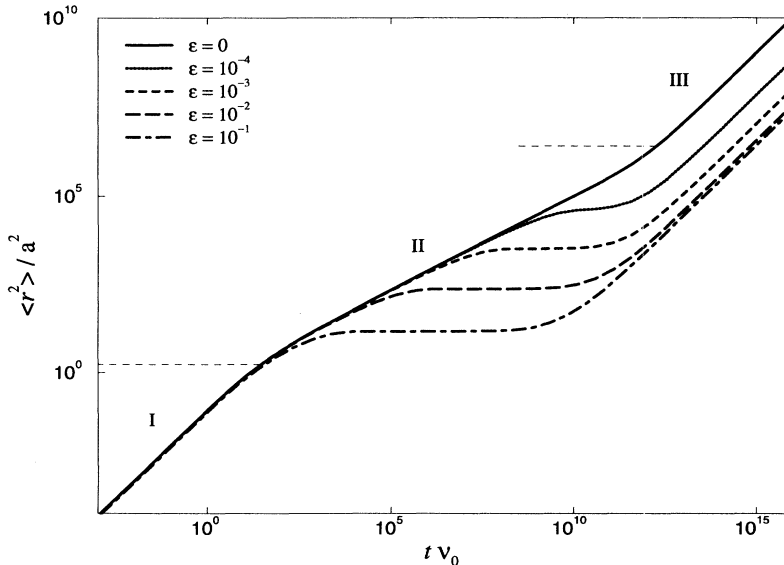


FIG. 6. MSD of a particle as a function of time on a square lattice with the distribution of barrier heights given in Eq. (17), for various  $\epsilon$  at constant  $k_B T = 0.033$ , as calculated by EMA; horizontal lines separate regions I, II, III in the case  $\epsilon = 0$ .

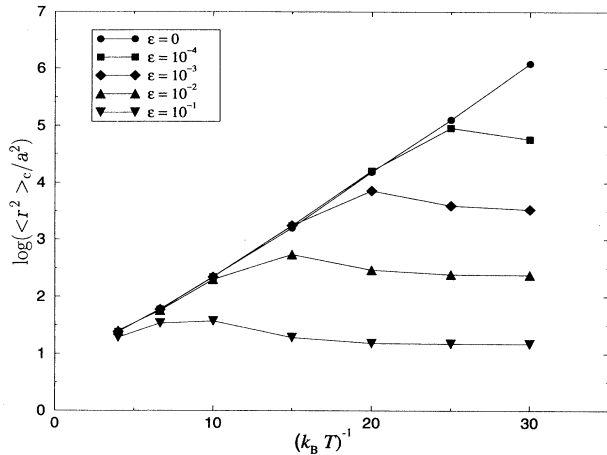


FIG. 7. Crossover MSD as a function of reciprocal temperature for diffusion on a square lattice with the distribution of barrier heights given in Eq. (17), for various  $\epsilon$ ; dots: calculated by EMA. Lines are guides for the eye.

this temperature-independent limit becomes the relevant crossover MSD. Solving Eq. (21) in the low-temperature limit ( $J_h/J_\epsilon \rightarrow 0$ , and  $J_l/J_\epsilon \rightarrow \infty$ ), the long-time effective jump frequency turns out to be

$$J_c^l = J_\epsilon \sim \exp[-E_\epsilon/(k_B T)]. \quad (28)$$

Thus, long-range diffusion is entirely controlled by the small concentration of defect barriers, and  $E_\epsilon$  is the activation energy of the long-time diffusion coefficient for low temperatures.

Concerning the dependence of critical crossover MSD on defect concentration, we obtain the relation

$$\langle r^2 \rangle_{c,d} \sim \epsilon^{-\beta} \quad (29)$$

with  $\beta \approx 1.2$ , from a comparison of the values of  $\langle r^2 \rangle_{c,d}$  for different  $\epsilon$  in the limit of low temperature. Since the long-time diffusion coefficient is independent of  $\epsilon$ , the crossover times show the same concentration dependence (29) as the crossover MSD.

In conclusion, we have described a kind of crossover

phenomenon, specifically, a transition from bulk-controlled to defect-controlled diffusion with decreasing temperature or increasing defect concentration.

#### IV. SUMMARY

We have presented a comparative study of particle diffusion in random-barrier models treated by Monte Carlo simulation and effective-medium approximation. Both methods were shown to agree well for the case of a box distribution of barrier heights on the square and on the simple-cubic lattice for a wide range of diffusion times and temperatures. The MSD undergoes a crossover from linear growth at short times (region I) to sublinear growth at intermediate times (region II) and back to linear behavior at long times (region III). This corresponds to a monotonous decrease of the diffusion coefficient, which is proportional to the arithmetical mean of jump frequencies in the beginning, and is then reduced to its long-time value by correlations between successive jumps. For a continuous distribution of barrier heights, the crossover from region II to region III occurs at an almost temperature-independent crossover MSD  $\langle r^2 \rangle_c$ . For a discrete distribution with a small concentration  $\epsilon$  of defect barrier heights at the percolation threshold, which was studied on the square lattice by EMA, there occurs a transition from bulk-controlled diffusion, characterized by temperature-dependent  $\langle r^2 \rangle_c$ , to defect-controlled diffusion with a crossover MSD that depends only on defect concentration, and a long-time diffusion coefficient that depends only on the defect barrier height.

#### ACKNOWLEDGMENTS

This project was supported by EU grant Copernicus, No. CIPA-CT93-0105. One of us, A.M., is indebted to Professor K. Binder for hospitality at the Institute of Physics, Johannes-Gutenberg University, Mainz, Germany during a stay supported by the Deutsche Forschungsgemeinschaft (DFG) under Grant No. 436-BUL-113/45.

[1] N. Wax, in *Selected Topics in the Theory of Noise and Stochastic Processes* (Dover, New York, 1954).  
 [2] J. Haus and K. W. Kehr, *Phys. Rep.* **150**, 263 (1987).  
 [3] V. Ambegaokar, B. F. Halperin, and J. S. Langer, *Phys. Rev.* **4**, 2612 (1971).  
 [4] I. Avramov, A. Milchev, and P. Argyrakis, *Phys. Rev. E* **47**, 2303 (1993).  
 [5] I. Avramov and A. Milchev, *J. Non-Cryst. Solids* **104**, 253 (1988).  
 [6] N.F. Mott, *Philos. Mag.* **19**, 835 (1969); *Festkörperprob-*

*leme* **9**, 22 (1969).  
 [7] T. Odagaki and M. Lax, *Phys. Rev.* **24**, 5284 (1981).  
 [8] S. Summerfield, *Solid State Commun.* **39**, 401 (1981).  
 [9] I. Webman, *Phys. Rev. Lett.* **47**, 1496 (1981).  
 [10] S. Kirkpatrick, *Rev. Mod. Phys.* **45**, 574 (1973).  
 [11] H. Ambaye and K. Kehr, *Phys. Rev. E* **51**, 5101 (1995).  
 [12] J. M. Luck, *Phys. Rev.* **43**, 3933 (1991).  
 [13] W. Schirmacher, *Solid State Ionics* **28**, 129 (1988).  
 [14] K. Mendelsson, *J. Appl. Phys.* **46**, 917 (1975).